

Graphical Synopsis

Inorganic Crystal Structures

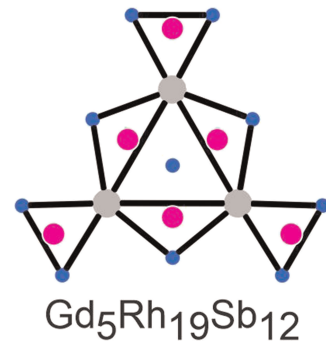
Inga Schellenberg, Theresa Block and Rainer Pöttgen

Gd₅Rh₁₉Sb₁₂ – a metal-rich antimonide with a Sc₅Co₁₉P₁₂ related structure

<https://doi.org/10.1515/zkri-2025-0017>

Z. Kristallogr. 2025; 240(9–10): 267–273

Synopsis: Gd₅Rh₁₉Sb₁₂ is the first antimonide with a Sc₅Co₁₉P₁₂ related structure. The crystal chemical difference concerns the ordering of the transition metal atoms on the *c* axis.



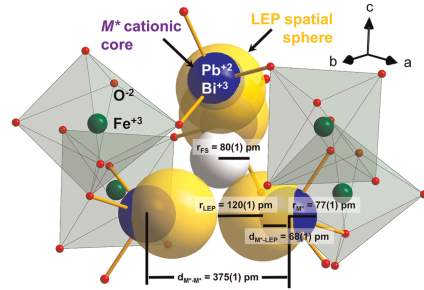
Carla M. Uribe-Rincón, Thorsten M. Gesing and Mohammad Mangir Murshed

Synthesis of schafarzikite-type (PbBi)(Fe_{1-x}Mn_x)O₄: a study on structural, spectroscopic and thermogravimetric properties

<https://doi.org/10.1515/zkri-2025-0023>

Z. Kristallogr. 2025; 240(9–10): 275–282

Synopsis: Crystal structure of (PbBi)FeO₄ schafarzikite, showing the edge-sharing FeO₆ octahedra chains and the distorted LO₃E tetrahedra (*L* = Pb, Bi; *E* = 6s² lone electron pair). The *L*-cation is decomposed into a cationic core (M^{*}) and a LEP spatial sphere with radius of r_{M*} and r_{LEP}, respectively, and d_{M*-LEP} refers to the distance between their centers. This representation also allows to estimate the free space with a radius of r_{FS} in the center of a pseudo-tetrahedron formed by four LEP cations, which fits well for small cations such as lithium.

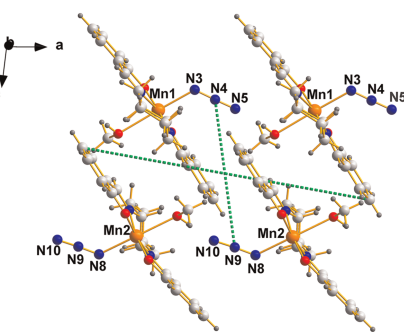


Demetrius C. Levendis and Ivan Bernal

Crystals of Racemic Mimics. Part II. Some Mn(III) and Co(III) compounds crystallizing thus, and remarks on the chirality of atoms containing non-bonded electron pairs as stereogenic centers

<https://doi.org/10.1515/zkri-2025-0012>
Z. Kristallogr. 2025; 240(9–10): 283–287

Synopsis: A quartet of molecules in GISXAK (II). The intersection of dotted lines marks one of the near-inversion centers always present in the contents of the unit cell of crystalline *Racemic Mimics*.

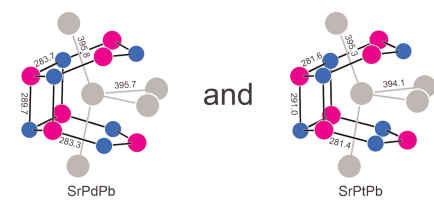


Lukas Heletta, Theresa Block and Rainer Pöttgen

The plumbides SrPdPb and SrPtPb

<https://doi.org/10.1515/zkri-2025-0040>
Z. Kristallogr. 2025; 240(9–10): 289–294

Synopsis: The equiatomic plumbides SrPdPb and SrPtPb crystallize with the orthorhombic TiNiSi-type structure, space group *Pnma*.

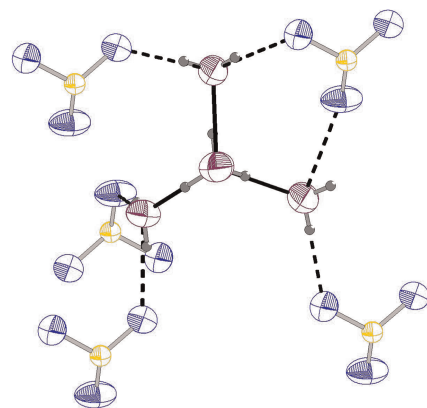


Tobias Lapić, David van Gerven, Rebecca F. Maier and Mathias S. Wickleder

In situ crystallization of the tetrahydrate of pentafluoro-benzenesulfonic acid, featuring the *Eigen* ion (H_9O_4^+)

<https://doi.org/10.1515/zkri-2025-0037>
Z. Kristallogr. 2025; 240(9–10): 295–299

Synopsis: The $(\text{H}_9\text{O}_4)^+$ ion has been characterized in the crystal structure of $(\text{H}_9\text{O}_4)[\text{C}_6\text{F}_5\text{SO}_3]$, the tetrahydrate of pentafluorobenzenesulfonic acid. Single crystals of the compound have been obtained by *in situ* crystallization on an X-ray diffractometer.



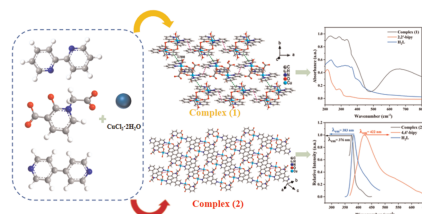
Organic and Metalorganic Crystal Structures

Yuzhu Song, Chang Xu, Tianyu Bai and
Xiuyan Wang

Two novel copper(II) supramolecular complexes: synthesis, crystal structures, and Hirshfeld surface analysis

<https://doi.org/10.1515/zkri-2025-0031>
Z. Kristallogr. 2025; 240(9–10): 301–310

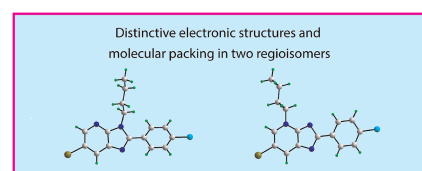
Synopsis: Reacting 3-carboxy-1-carboxymethyl-2-oxidopyridinium (H_2L) and N-donor ligands (2,2'-bipy, 4,4'-bipy) with Cu(II) ions yielded two complexes: biaqua-bis [$[\mu_2\text{-}3\text{-carboxylato-1-carboxylatomethyl-2-oxidopyridinium-}\kappa^3\text{O,O':O''}]\text{-}(2,2'\text{-bipyridine-}\kappa^2\text{N,N'})$ copper(II)] tetrahydrate (**1**) and poly{aqua- $[\mu_2\text{-}3\text{-carboxylato-1-carboxylatomethyl-2-oxidopyridinium-}\kappa^3\text{O,O':O''}]\text{-hemi}(\mu_2\text{-}4,4'\text{-bipyridine-}\kappa^2\text{N:N'})$ copper(II)} bihydrate (**2**). In (**1**), the anionic H_2L links Cu(II) to form $[\text{Cu(L)}_2]$ units, which ultimately form supramolecular layers through two different types of $\pi\text{-}\pi$ stacking interactions of 2,2'-bipy. In (**2**), binuclear $[\text{Cu(L)}_2]$ moieties form chains via 4,4'-bipy bridging, further connected by H-bonds into a layered structure. Both complexes were characterized using FT-IR, UV-vis, PL, TG, and Hirshfeld surface analyses.



Selma Bourichi, Khalid Boujdi,
Rachida Amanarne, Younes Ouzidan,
Youssef Kandri Rodi, Fouad Ouazzani Chahdi,
Sang Loon Tan and Edward R. T. Tiekkink
6-Bromo-3-butyl-2-(4-chlorophenyl)-3H-imidazo[4,5-b]pyridine and its 4-butyl regioisomer: synthesis and analysis of supramolecular assemblies

<https://doi.org/10.1515/zkri-2024-0120>
Z. Kristallogr. 2025; 240(9–10): 311–324

Synopsis: Rather distinct electronic structures are evident in the regioisomeric structures which differ in the location of the imidazoyl- or pyridyl-bound n-butyl substituents.



Subrata Ranjan Dhara, Purak Das, Suven Das and Arpita Dutta

Synthesis, crystal structure, and Hirshfeld analysis of an ultrashort hybrid peptide

<https://doi.org/10.1515/zkri-2025-0022>

Z. Kristallogr. 2025; 240(9–10): 325–332

Synopsis: In the present study, an ultrashort hybrid peptide, namely, Boc-L-Pro-5-AIA(OMe)₂ was synthesized, where 5-amino isophthalic acid (5-AIA) was employed as a rigid non-coded aromatic α -amino acid. The single crystal X-ray diffraction analysis revealed that L-Pro induced a turn in the molecular conformation. Two hybrid peptide molecules are assembled in an antiparallel criss-cross fashion and interlocked by hydrogen bonding interactions, resulting in a robust dimer. Interestingly, the dimers are self-assembled to a unique water-mediated sheet network. The classical and non-classical interactions played a crucial role in the stability of the crystal packing, which are supported by Hirshfeld surface and 2D fingerprint analysis.

